



# Origin of warm springs in Banks Peninsula, New Zealand



Sammy Griffin <sup>a</sup>, Travis W. Horton <sup>a, \*</sup>, Christopher Oze <sup>b</sup>

<sup>a</sup> Department of Geological Sciences, University of Canterbury, Private Bag 4800, Christchurch 8041, New Zealand

<sup>b</sup> Department of Geology, Occidental College, 1600 Campus Rd., Los Angeles, CA 90041, USA

## ARTICLE INFO

### Article history:

Received 27 April 2017

Received in revised form

14 September 2017

Accepted 18 September 2017

Available online 21 September 2017

Handling editor: Dr. I. Cartwright.

### Keywords:

Hydrothermal system

Soil gas flux

Isotope geochemistry

Warm springs

Volcanic province

Earthquake perturbation

## ABSTRACT

Thermal springs present rare opportunities to locate and interpret the geological drivers of upper-crustal fluid flow. Interpreting the conditions through which crustal fluids are heated and released to the surface is important for advancing our understanding of crustal deformation and geothermal resource potential across tectonic contexts. In New Zealand, the majority of thermal springs are associated with magmatic-hydrothermal systems in the central North Island or with the rapidly uplifting bedrock in the South Island's convergent fault systems. However, low enthalpy systems outside of these areas represent attractive targets for potential geothermal resource development. The low enthalpy warm springs of Banks Peninsula, located immediately adjacent to Christchurch, represent a highly understudied but potentially significant resource to the South Island's most densely populated metropolitan area. Hosted within the eroded 11–5.8 Ma volcanic complex of Banks Peninsula, these warm springs (14.5–33.6 °C) represent an anomalous hydrothermal system that has been perturbed by the 2010–2016 Canterbury Earthquake Sequence (CES). The February 22, 2011, Mw 6.2 earthquake induced observable changes to the Banks Peninsula warm springs system, including the appearance of new warm springs within the peninsula's north-western Hillsborough Valley. We assess the origins of the volcanically-hosted Banks Peninsula warm springs post-CES using an integrated isotopic, geochemical, and soil gas flux approach. Additionally, we elucidate the tectonic context and geological drivers of upper-crustal fluid flow in the Banks Peninsula warm spring system. Aqueous phase emissions from the springs predominantly plot within the  $\text{Na}^+ + \text{K}^+/\text{HCO}_3^-$  type waters and exhibit  $\delta^{18}\text{O}$ ,  $\delta\text{D}$ , and  $\delta^{13}\text{C}$  values of  $-8.30$  to  $-9.26\%$  V-SMOW,  $-60.15$  to  $-64.19\%$  V-SMOW, and  $-12.37$  to  $-15.06\%$  V-PDB, respectively. Soil gas flux surveys of the springs at Rapaki Bay revealed  $\text{CO}_2$  fluxes that average  $6.93 \pm 10 \text{ gm}^{-2} \text{ day}^{-1}$ , with an average  $\delta^{13}\text{C}$  value of  $-19.81 \pm 5\%$  V-PDB, and  $\text{CH}_4$  fluxes that average  $5.58 \pm 12 \text{ gm}^{-2} \text{ day}^{-1}$ , with an average  $\delta^{13}\text{C}$  value of  $-59.52 \pm 1\%$  V-PDB. Our results suggest that the Banks Peninsula warm springs are a structurally controlled, upper-crustal metamorphic hydrothermal heated system, sourced from high-altitude Southern Alps derived meteoric waters. Carbon isotope compositions of gaseous emissions associated with the Banks Peninsula thermal springs are consistent with an upper-crustal metamorphic decarbonation and decarboxylation carbon source. Based on their geochemistry, we propose that the Banks Peninsula warm springs should be considered an outboard extension of the South Island's plate-boundary hydrothermal system. Such connectivity implies that long-lived low-enthalpy geothermal resources may be associated with permeable and distributed fault networks in the periphery of convergent margins.

© 2017 Published by Elsevier Ltd.

## 1. Introduction

Hydrothermal systems have been shown to be a major contributing factor to the development of geological faults and processes which influence earthquake rupture cycles (e.g.,

Sutherland et al., 2017), and tectonic-hydrothermal systems represent potentially attractive low-enthalpy geothermal resource targets (e.g., Guglielmetti et al., 2013). Many similar systems, associated with active deformation along the Australian-Pacific plate boundary, are present on New Zealand's South Island (Fig. 1A; Beyssac et al., 2016; Cox et al., 2015; Horton et al., 2001; Menzies et al., 2016; Reyes et al., 2010). However, the geological drivers behind the presence of warm springs on Banks Peninsula,

\* Corresponding author.

E-mail address: [travis.horton@canterbury.ac.nz](mailto:travis.horton@canterbury.ac.nz) (T.W. Horton).

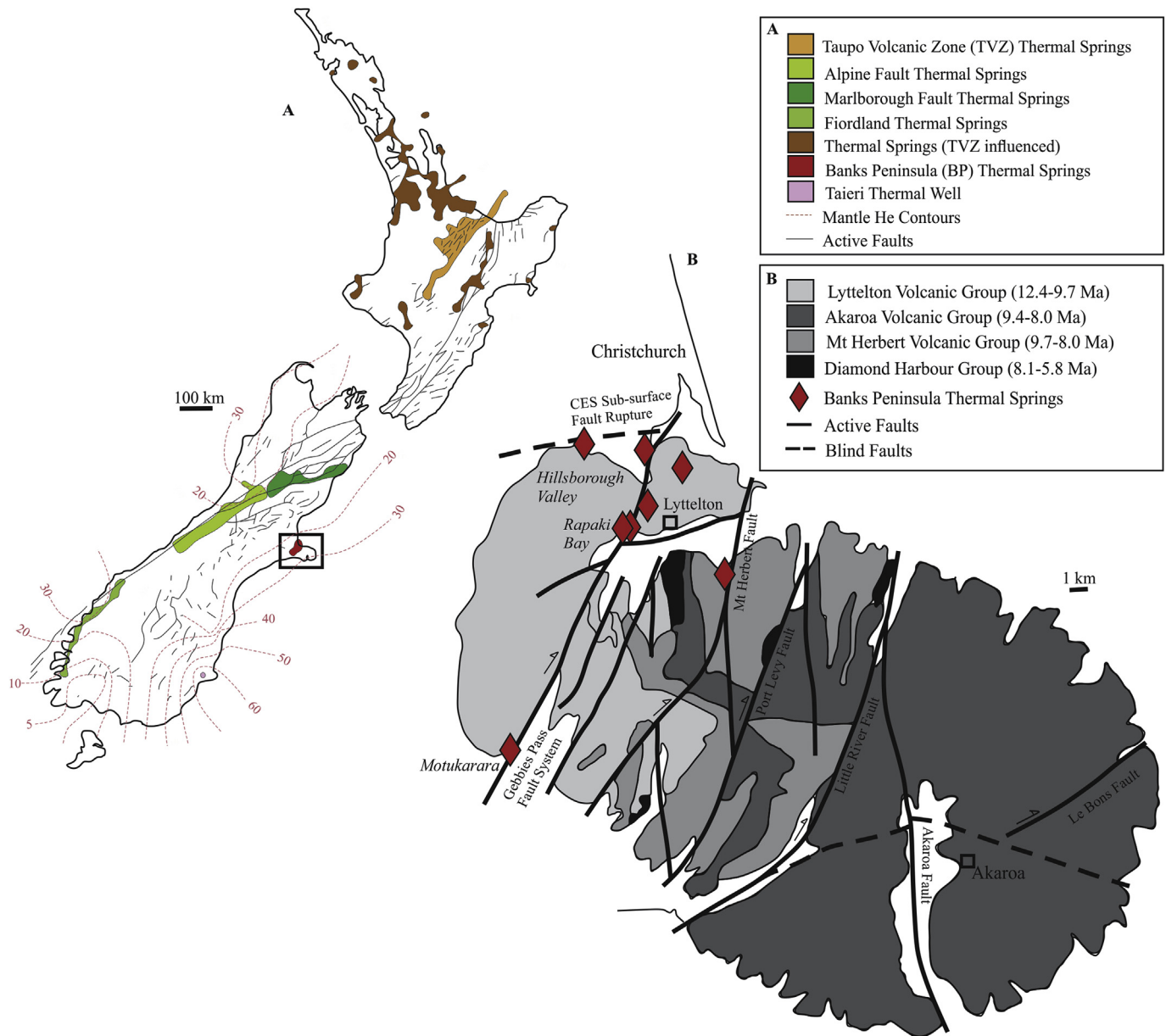


**Fig. 1.** A) Location of study area within the national hydrothermal context of New Zealand. Banks Peninsula (outlined) in the context of mantle He (Hoke et al., 2000). B) Simplified local geology and location of previously reported warm springs of the Banks Peninsula area. Hillsborough Valley, Rapaki Bay, and Motukarara indicate the sample sites of this study.

east coast South Island, remain unknown (Reyes and Jongens, 2005).

Despite the highly eroded Banks Peninsula being comprised of four geochemically distinct volcanic groups (Brown and Weeber, 1994; Hampton et al., 2012; Sewell et al., 1992), the area's warm springs are only observed along the Mt Herbert fault (dextral strike-slip), Gebbies Fault system (normal) and from hydrogeological effects of the Canterbury Earthquake Sequence (CES) subsurface fault rupture (reverse; Fig. 1B). These deformational systems are located within the structurally controlled trachytic-basaltic Lyttelton Volcanic Group (11–9.7 Ma; Beavan et al., 2011; Hampton, 2010; Ring and Hampton, 2012) and are considered to be related to the larger regional Canterbury Horst structure of the deformed slightly metamorphosed argillite and greywacke torlesse of the Rakaia terrane (Forsyth et al., 2008; Ring and Hampton, 2012; Sewell et al., 1992). The Rakaia terrane, which directly underlies the Lyttelton

Volcanic Group and encompasses a large section of the South Island including sections of the Southern Alps, is known to host thermal waters that are driven by structural controls directly related to the South Island's plate-boundary system (Barnes et al., 1978; Craw et al., 2013; Horton et al., 2001).

The February 22, 2011, Mw 6.2 earthquake subsurface fault rupture occurred beneath the northwestern flank of Banks Peninsula (Forsyth et al., 2008; Kaiser et al., 2012; Mortimer, 2004; Quigley et al., 2016). Associated effects of this major seismic event include: 1) establishment of groundwater springs in the north-western Hillsborough Valley; and 2) increased activity and localised expansion of pre-existing warm springs at Rapaki Bay and Motukarara (Fig. 1B; Green, 2015; Griffin, 2016; Kaiser et al., 2012). The hydrogeological effects of the CES present a unique opportunity to describe and interpret the upper-crustal fluid flow system responsible for these springs. Here, we utilise aqueous

**Table 1**  
Geochemical analysis of selected Banks Peninsula warm springs.

Locality	Motukarara				Rapaki Bay				Hillsborough Valley		Rain Water	Ocean Water	Blank
Sample	MS1	MS2	RBS1	RBS2	RBS3	RBS4	RBS5	HVS1	HVS2	RBR	RBO	Blank	
Coordinates	43 °43'22.58"S 172 °35'42.38"E	43 °31'22.43"S 172 °35'42.51"E	43 °36'27.26"S 172 °41'1.34"E	43 °36'27.30"S 172 °41'2.36"E	43 °36'27.34"S 172 °41'2.60"E	43 °36'27.42"S 172 °41'2.85"E	43 °36'27.34"S 172 °41'4.34"E	43 °33'57.92"S 172 °39'41.59"E	43 °33'44.34"S 172 °39'17.51"E	43 °36'27.20"S 172 °41'4.76"E	–	–	
Temperature °C	18.0	17.0	30.4	33.6	28.6	30.2	32.0	14.5	18.3	6.0	7.7	6.0	
pH	7.5	7.7	8.4	8.2	8.2	8.2	8.2	7.7	7.5	6.9	8.1	N.D.	
Conductivity µS/cm	678.030	650.050	1170.870	1168.830	7549.030	3441.610	1199.310	1193.800	1106.640	281.980	41312.810	N.D.	
Total Alkalinity mg/L	249.300	221.100	922.900	931.300	915.200	936.700	959.800	106.600	107.000	10.000	49.200	N.D.	
F mg/L	0.156	0.144	2.898	3.001	2.577	2.945	2.945	0.236	0.229	0.122	0.304	0.001	
Cl mg/L	122.947	116.512	236.300	235.832	1703.376	242.842	242.842	241.575	221.527	31.855	9468.946	0.008	
Br mg/L	0.293	0.278	0.442	0.652	5.125	0.669	0.669	0.562	0.375	B.D.	40.585	0.030	
NO <sub>3</sub> mg/L	0.476	0.209	B.D.	B.D.	0.074	B.D.	B.D.	5.100	3.010	0.446	59.942	0.026	
SO <sub>4</sub> mg/L	13.984	13.366	0.349	1.870	214.267	77.570	1.400	44.868	35.243	5.557	2491.199	0.001	
PO <sub>3</sub> mg/L	3.864	3.102	4.352	4.635	5.275	5.525	6.672	3.041	3.472	5.741	6.434	0.001	
Na mg/L	111.390	104.871	489.880	494.879	1313.340	571.540	487.182	151.617	114.993	16.571	N.D.	0.030	
Mg mg/L	12.599	11.391	9.609	9.970	116.917	18.184	9.305	30.762	25.004	2.031	N.D.	0.001	
Al mg/L	0.009	0.016	0.019	0.031	0.037	0.029	0.014	0.015	0.010	0.103	N.D.	0.001	
K mg/L	2.841	2.638	19.997	20.374	49.368	22.059	20.011	4.455	3.516	0.845	N.D.	0.005	
Ca mg/L	17.821	18.205	15.210	14.818	59.606	9.936	15.343	49.861	35.871	1.967	N.D.	0.033	
V µg/L	18.527	18.159	0.721	3.080	3.462	1.019	0.135	3.008	8.619	0.353	N.D.	0.011	
Cr µg/L	B.D.	0.005	0.264	B.D.	0.403	B.D.	B.D.	0.401	0.444	4.505	N.D.	0.030	
Mn µg/L	B.D.	B.D.	70.666	89.514	85.880	49.601	10.843	1.643	14.538	11.533	N.D.	B.D.	
Fe µg/L	17.208	13.962	177.782	110.505	245.531	159.032	225.082	39.587	97.000	95.032	N.D.	0.302	
Co µg/L	B.D.	B.D.	0.001	0.060	0.006	0.044	B.D.	0.003	B.D.	0.305	N.D.	B.D.	
Ni µg/L	B.D.	B.D.	B.D.	0.002	B.D.	B.D.	B.D.	0.070	B.D.	1.708	N.D.	0.022	
Cu µg/L	0.36	0.183	0.486	0.400	0.359	0.475	0.438	0.253	0.016	15.497	N.D.	0.356	
Zn µg/L	5.643	14.492	8.621	4.078	23.034	8.594	3.533	4.100	4.214	421.578	N.D.	1.286	
As µg/L	0.574	0.665	3.635	6.609	8.267	3.084	1.810	1.347	1.264	2.284	N.D.	0.020	
Cd µg/L	0.042	0.020	0.016	0.053	0.138	0.012	0.021	0.064	0.058	1.695	N.D.	0.009	
Sb µg/L	0.797	0.686	0.462	0.401	0.908	33.40	0.399	1.797	1.082	0.764	N.D.	0.045	
Pb µg/L	0.104	0.036	0.069	0.189	0.399	0.131	0.053	0.249	0.056	1.444	N.D.	0.017	
Na:Cl	4:3	4:3	3:1	3:1	1:1	7:2	3:1	1:1	4:5	4:5	–	4:1	
C mMol/L	4.086	3.624	3.566	2.843	3.101	3.427	3.602	1.747	1.754	0.164	3.974	N.D.	
DIC <sup>-1</sup>	0.245	0.276	0.280	0.352	0.322	0.292	0.278	0.572	0.570	6.101	0.252	N.D.	
δ <sup>13</sup> C (DIC) ‰ V-PDB	-13.35 ± 0.02	-13.52 ± 0.3	-12.76 ± 0.1	-12.44 ± 0.1	-12.37 ± 0.08	-12.41 ± 0.1	-12.70 ± 0.09	-15.56 ± 0.1	-14.82 ± 0.02	-8.62 ± 0.02	-1.22 ± 0.06	N.D.	
δ <sup>18</sup> O (DIC) ‰ V-PDB	-11.42 ± 0.3	-11.46 ± 0.2	-11.90 ± 0.1	-12.62 ± 0.2	-12.89 ± 0.09	-11.99 ± 0.1	-12.46 ± 0.06	-10.36 ± 0.4	-11.39 ± 0.2	-10.92 ± 0.00	-5.58 ± 0.1	N.D.	
δ <sup>18</sup> O (H <sub>2</sub> O) ‰ V-SMOW	-8.44 ± 0.1	-8.40 ± 0.05	-9.46 ± 0.07	-9.26 ± 0.2	-8.86 ± 0.1	-8.98 ± 0.2	-9.26 ± 0.06	-8.63 ± 0.06	-8.30 ± 0.08	-6.95 ± 0.06	N.D.	N.D.	
δD (H <sub>2</sub> O) ‰ V-SMOW	-61.35 ± 0.3	-61.85 ± 0.03	-64.04 ± 0.9	-64.19 ± 1	-60.15 ± 0.3	-62.14 ± 0.6	-62.97 ± 0.2	-61.95 ± 0.2	-62.14 ± 0.3	-42.85 ± 0.4	N.D.	N.D.	
d-excess	6.19	5.33	11.60	9.88	10.74	9.67	11.10	7.08	4.27	12.76	N.D.	N.D.	

B.D.below detection, N.D. no data, DIC dissolved inorganic carbon.



geochemistry in conjunction with novel soil gas flux surveying methods to elucidate the fluid flow conditions in the anomalous and understudied low enthalpy warm spring system situated within the Lyttelton volcanics of Banks Peninsula, New Zealand.

## 2. Materials and methods

Nine warm springs were analysed at three locations and were compared with previous recorded warm spring data (Table 1, Fig. 1B; Brown and Weeber, 1994; Forsyth et al., 2008; Reyes et al., 2010; Reyes and Britten, 2007; Sewell et al., 1992; Thain et al., 2006). Sample sites were selected based on their anecdotal reported expansion/appearance following the 2011 Canterbury Earthquake Sequence. The warm springs were identified using a FLIR ONE infrared camera attached to an Apple I-Phone 5 (Fig. 2). Site coordinates were recorded using a Garmin GPSmap 62S GPS.

Individual water samples were collected June 2015. Additional ocean (RBO), meteoric (RBR), blank, and duplicate (RBS3D) samples were taken at Rapaki Bay for comparison and quality control. Filtered and unfiltered samples were taken from each spring at the point source using sterile Chirana 20 ml Luer syringes and placed into new and sample rinsed 15 ml centrifuge tubes. 0.45  $\mu$ l sterile Millex HA filter unit MF-milipore MCE membrane syringe filters were used to filter samples. Trace metal and cation samples were then acidified with 10  $\mu$ l of 70% ultrapure nitric acid at a clean room at the University of Canterbury Chemistry Department. Conductivity ( $\mu$ S/cm) and pH were analysed using a Mettler Toledo SevenGo Duo pro pH/Ion/Cond with meter heads, Mettler Toledo Inlab<sup>®</sup> Expert Pro-ISM-IP67 pH 0–14, 0–100 °C and Mettler Toledo Inlab<sup>®</sup> 738 ISM Conductivity NTC 30 k $\Omega$  0.01–1000 mS/cm, 0–100 °C. Water temperature was measured *in situ* by a Centre 370 RDT thermometer ( $\pm 0.1$  °C).

Anions including F<sup>-</sup>, Cl<sup>-</sup>, Br<sup>-</sup>, NO<sub>3</sub><sup>-</sup>, SO<sub>4</sub><sup>2-</sup>, and PO<sub>3</sub><sup>2-</sup> were analysed from filtered samples using a reagent-free DIONEX RF-IC 2100 Ion Chromatograph (IC) at the University of Canterbury. Species concentration was determined from comparison against 0.1, 1.0, 5, 25, 50, 100 mg/l calibration standards. Total alkalinity (HCO<sub>3</sub><sup>-</sup><sub>(aq)</sub>) was measured in the field and the collected data was processed with the USGS alkalinity calculator using both the Inflection Point and Gran method for comparison (USGS, 2013, 2012).

Both filtered and unfiltered samples were analysed for major elements (K<sup>+</sup>, Na<sup>+</sup>, Al<sup>3+</sup>, Mg<sup>2+</sup> and Ca<sup>2+</sup>) and trace metals (V, Cr, Mn, Fe, Co, Ni, Cu, Zn, As, Cd, Sb, and Pb) using the Agilent 7500 Series Inductively Coupled Plasma Mass Spectrometer (ICP-MS) with Octopole Reaction System at the University of Canterbury. Samples underwent 21  $\times$  dilution in 10 ml 2% HNO<sub>3</sub> prior to analysis. Exceptions include the RBS3 and RBS4 samples which underwent 51  $\times$  dilution in 10 ml 2% HNO<sub>3</sub> due to their elevated chloride concentrations (identified by the IC results) and the RBR and blank samples which were undiluted. The unfiltered and filtered blanks, taken in the field, were run alongside the duplicate (RBS3D) sample for quality control.

$\delta^{18}\text{O}$  and  $\delta\text{D}$  in water were analysed using a Picarro Liquid Isotope Analyser (LWIA) 1000 series at the University of Canterbury Stable Isotope Laboratory. For each sample, six injections of 2  $\mu$ m fluid were analysed using the LWIA. The first two injections were disregarded due to the memory effect. The mean and standard deviation were taken from the remaining four injections.  $\delta^{18}\text{O}$  and  $\delta\text{D}$  were normalised relative to replicate analysis of V-SMOW2 and SLAP (Southern Latitude Antarctic Precipitation) certified reference waters supplied by the International Atomic Energy Agency.  $\delta^{13}\text{C}$  and DIC concentration in water was analysed using a Thermo Finnigan Gas Bench II connected to a Thermo Finnigan Delta V+ isotope ratio mass spectrometer operating under continuous flow of ultra-high purity helium using the method described by Spötl

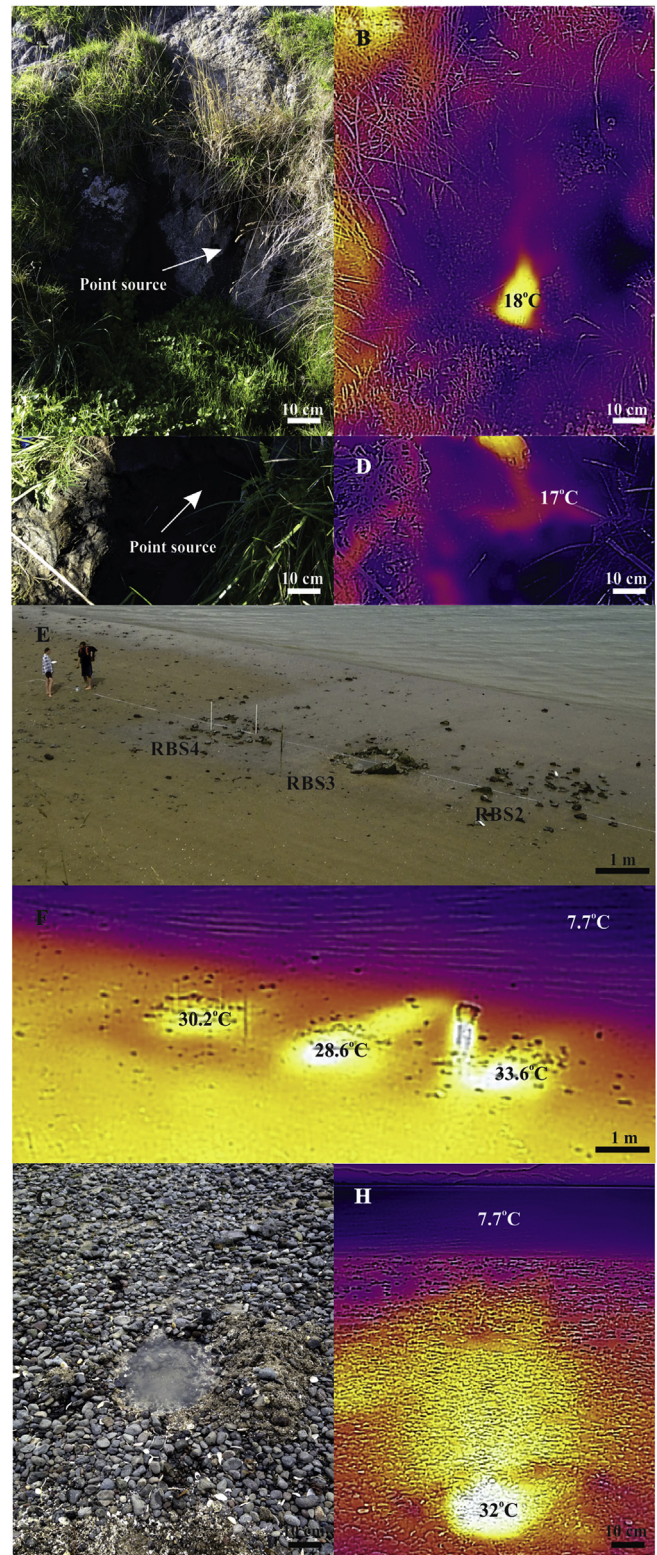


**Fig. 2.** Banks Peninsula warm springs. The Motukarara springs flow from the basaltic face of the Lyttelton volcanics at an extremely low flow rate. A) MS1 the pre-CES established spring; B) MS1 in infrared; C) MS2 formed post-CES; D) MS2 in infrared. The Rapaki Bay warm springs diffuse through the local sand with low flow rates E) RBS2–4 looking east towards the harbour. The three central springs sit between the high and low tide marks, RBS1 sits at the low tide mark (out of frame to the left of RBS2) and RBS5 sits above the high tide mark (out of frame to the right of RBS4). RBS3 is the only spring identified prior to the CES with all other identified springs identified post-CES; F) RBS2–4 in infrared, water from the springs can be seen flowing towards the ocean; G) RBS5 situated above the high tide mark facing south east; H) RBS5 in infrared facing south-east, water from the spring can be seen flowing towards the harbour.

(2005).  $\delta^{13}\text{C}$  values were normalised to V-PDB using replicate analysis of NBS-19 and NBS-22 certified reference materials. Stable carbon isotope compositions are both accurate and precise to  $<0.10\text{‰}$ .

Two soil gas surveys were undertaken at the Rapaki Bay site (25/03/2015 and 22/01/2016; Fig. 2E). Soil temperature was taken at 10 cm depth using a Centre 370 RDT thermometer ( $\pm 0.1\text{ °C}$ ). Soil gas flux measurements were taken according to the accumulation method adapted from Chiodini et al. (1998) (Griffin, 2016; Matt Hanson *pers. comm.*) using a combined West systems LI-COR 820 infrared  $\text{CO}_2$  gas analyser (IRGA) equipped with a WS-HC-IR  $\text{CH}_4$  ( $\text{g}$ ) detector, a  $\text{H}_2\text{S}$  detector and 1000 SCCM pump and a Picarro G2201-i  $\text{CO}_2$  and  $\text{CH}_4$  isotopic Cavity Ring Down Spectroscopy (CRDS) with additional SSIM2 and modified re-circulating pump (standard flow rate 25 SCCM) henceforth referred to as IRGA-CRDS (Griffin, 2016). The accumulation chamber used was an A type West Systems accumulation chamber with a cross sectional area of  $3.140 \times 10^{-2}\text{ m}^2$ , an internal volume of  $2.756 \times 10^{-3}\text{ m}^3$  that contained an appropriate vent, butyl rubber septa for discrete sampling, and a mixing vane surrounded by a modified shrub-tub

which acted as a skirt. Fluxes were determined over a 5 minute period with measurements above 0.1 ppm deemed as a positive flux (Griffin, 2016). Air temperature readings were provided from the New Zealand MetService Lyttelton Harbour weather station (ca. 2.5 km from sample location). Collected data was processed using a code written in the Freeware R (Matt Hanson *pers. comm.*) and interpreted through the GoldenSoftware computer program Surfer version 11 as discussed by Griffin (2016).

The IRGA is calibrated annually with a sensitivity range of 0–20,000 ppm ( $\text{CO}_2$ ), a 0–10,000 ppm sensitivity range for  $\text{CH}_4$ ; with a detection limit of 60 ppm, and has an  $\text{H}_2\text{S}$  sensitivity range of 0–25 ppm; with a detection limit of 0.02 ppm. Company precision of the flux is reported at 3%, but has been reported in the literature as  $\pm 10\%$  for flux ranging  $0.2\text{--}200\text{ gm}^{-2}\text{ day}^{-1}$  (Chiodini et al., 1998; Hanson et al., 2014) and  $\pm 5\%$  for fluxes greater than  $200\text{ gm}^{-2}\text{ day}^{-1}$  (Hanson et al., 2014). The CRDS has a company guaranteed precision of  $<1\%$  for concentrations up to 500 ppm;  $<0.5\%$  for concentrations 500–1500 ppm; and  $<0.2\%$  for concentrations 1500–3000 ppm and a maximum detection limit of 7000 ppm ( $\sim 300\text{ gm}^{-2}\text{ day}^{-1}$  with the given size of the accumulation chamber;

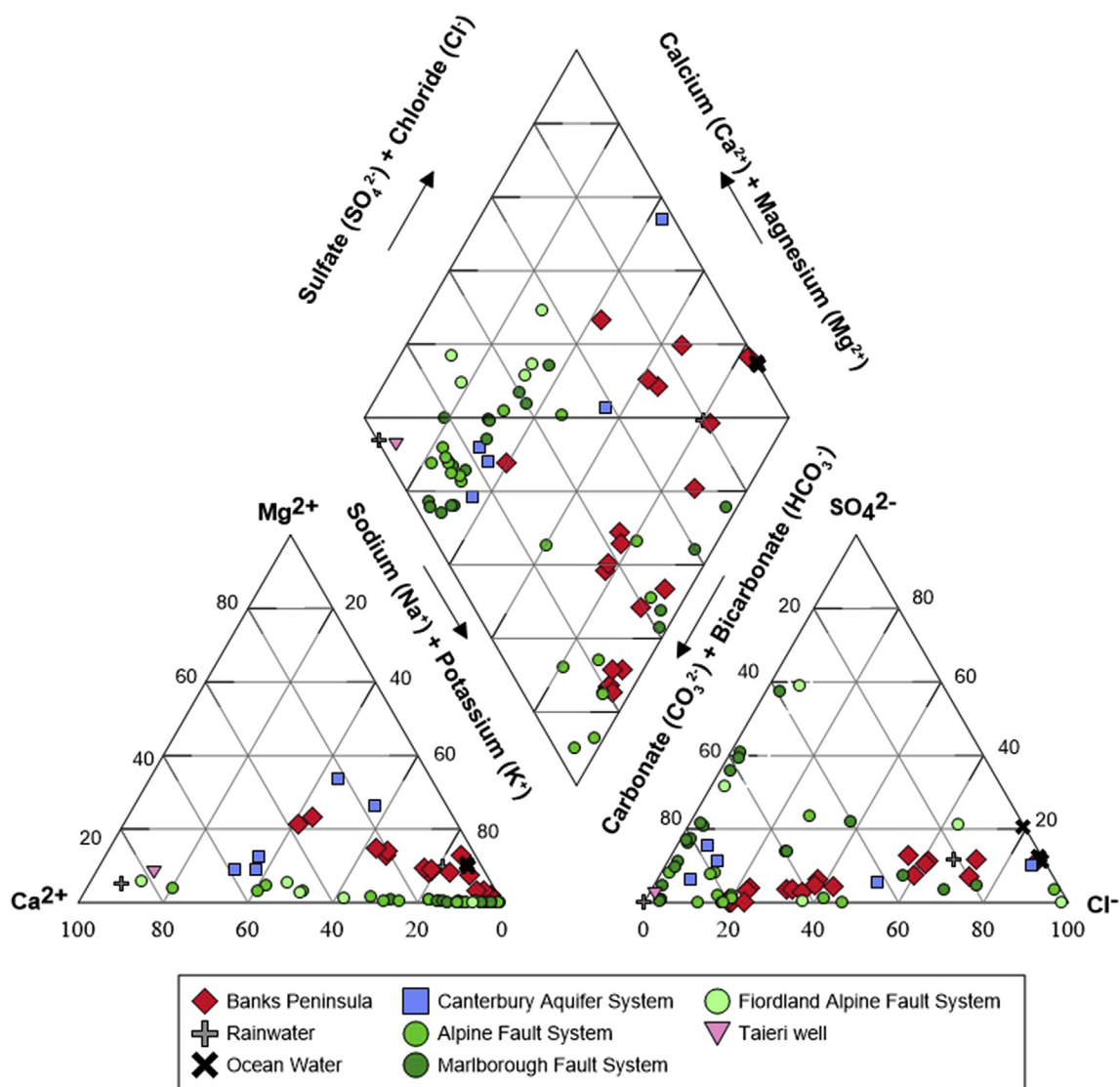


Fig. 3. Piper plot of South Island hydrothermal waters (Supplementary data from: Barnes et al., 1978; Brown et al., 1995; Cox et al., 2015; Green, 2015; Hayward, 2002; Menzies et al., 2016; Reyes et al., 2010; Scott, 2014; Stewart, 2012).



Matt Hanson *pers. comm.*). CRDS fluxes are reported to be 102% of the traditional soil gas flux meter values (Matt Hanson *pers. comm.*). The CRDS was calibrated daily via running 4 psi standard gas for 40 minutes prior to and post sampling.

### 3. Results and discussion

#### 3.1. Water analyses: major elements, trace elements, and pH

To date, studies have considered the Banks Peninsula warm springs to exhibit waters controlled by the deep-seated remnants of the alkaline volcanic provenance. The warm springs waters at Banks Peninsula exhibit pH values ranging from 7.5 to 8.4. These values are more alkaline than local rain (pH 6.9; Table 1), but are still well within the ranges recorded at other South Island hydrothermal springs (Barnes et al., 1978; Cox et al., 2015; Reyes et al., 2010). The Banks Peninsula hydrothermal system predominantly exhibits  $\text{Na}^+ + \text{K}^+/\text{HCO}_3^-$  type waters (Fig. 3). Some of the springs, associated with the Birdlings Flat loess (Hillsborough Valley; Fig. 1), plot within the  $\text{Na}^+ + \text{K}^+/\text{Cl}^-$  region. This distinct chemical signature in part results from excess chloride leaching from the high salt concentrated Birdlings Flat loess (Griffiths, 1973); which infills the lower regions and valleys surrounding Banks Peninsula, particularly on the northeastern flank. A shift toward the Pleistocene

hosted Canterbury Aquifer System (CAS) is also observed for some of these  $\text{Na}^+ + \text{K}^+/\text{Cl}^-$  springs reflecting some mixing between the warm springs and the neighbouring aquifer system waters. These particular springs also show lower temperatures (14.5–18.3 °C; with local groundwater being 11 °C); compared to the other sampled warm springs (28.6–33.6 °C; Table 1; *n.b.* That the HVS1-2 samples could not be taken at the point source due to obstruction from the residential buildings). The waters from the Banks Peninsula warm springs exhibit a distinct chemical difference from the sampled local rain and ocean water. The RBS3 sample exhibits signs of salt water contamination and the local rain sample (RBR) exhibits contamination from local sea spray that is unidentifiable within the other samples (Figs. 4 and 5; Table 1; Griffin, 2016). The elemental and trace metal concentrations from the water samples presented in this study indicate the Banks Peninsula warm springs to consist of unequilibrated and immature waters that exhibit minor amounts of water-rock interaction. The chemical signature, particularly within the trace metal concentrations indicates the water-rock interaction to be with the underlying Rakaia terrane rather than the overlying Lyttelton Volcanic Group or the neighbouring Pleistocene and Cenozoic sediments of the Canterbury plains (Barnes et al., 1978; Cox et al., 2015; Craw et al., 2013; Griffin, 2016; Horton et al., 2001; Menzies et al., 2016; Reyes et al., 2010; Scott, 2014; Stewart, 2012).

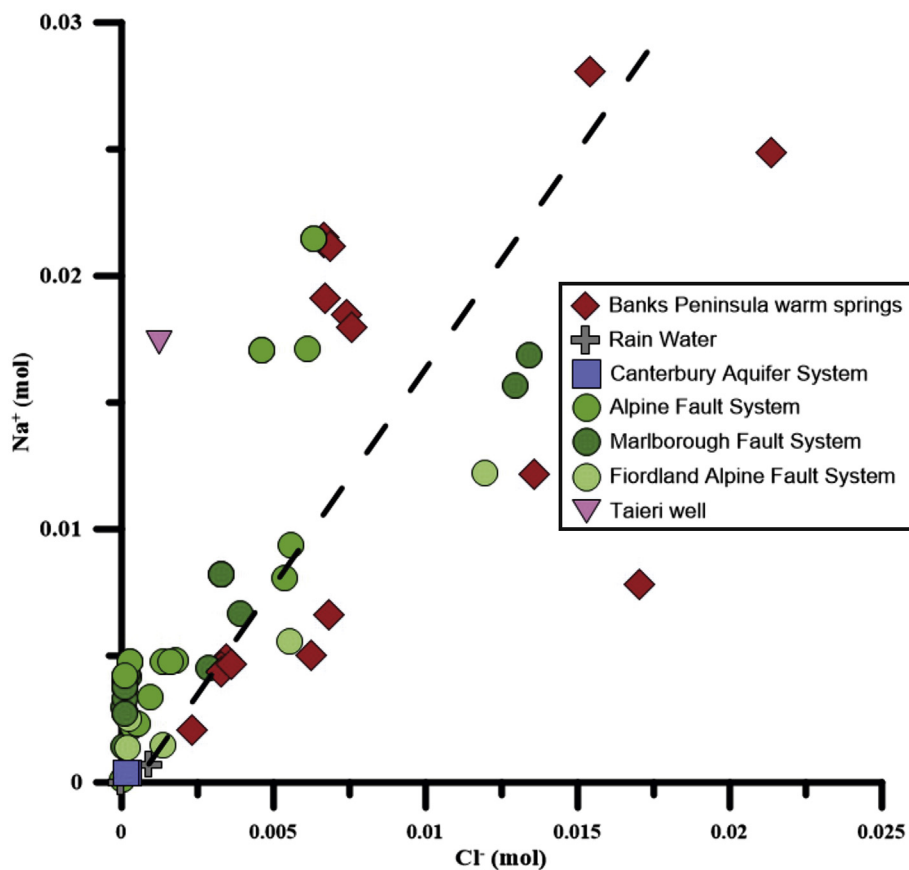


**Fig. 4.** Rain-salt water influence of South Island hydrothermal waters. The Banks Peninsula warm springs (red) exhibit high concentrations of dissolved  $\text{Na}^+$  and  $\text{Cl}^-$ . These high concentrations are not necessarily indicative of salt water influence with many other studied Southern Alps based hydrothermal springs (green) also exhibiting similar concentrations with no feasible salt water influences. Samples taken from the Hillsborough valley region are easily identified by their high  $\text{Cl}^-$  concentrations resulting from interaction with the surrounding Birdlings Flat loess (Griffin, 2016). The highest concentrated Banks Peninsula spring (RBS3, Table 1) exhibits signs of salt water contamination (Griffin, 2016). All of the identified South Island thermal springs plot along the rainwater-ocean water mixing line (dashed). The springs exhibit a different geochemical signature to the only other known South Island volcanic hosted thermal well (Taieri). (Supplementary data from: Aitchison-Earl et al., 2003; Barnes et al., 1978; Cox et al., 2015; Environment Canterbury, 2014; Hayward, 2002; Reyes et al., 2010). (For interpretation of the references to colour in this figure legend, the reader is referred to the web version of this article.)

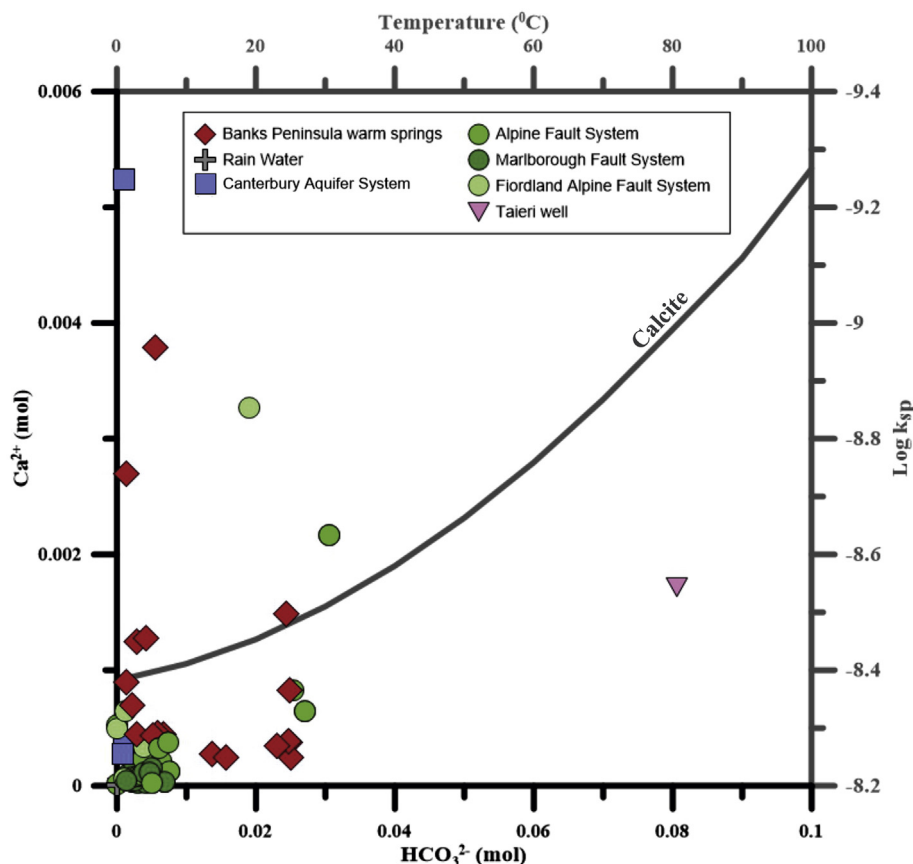


**Fig. 5.** Dissolved calcite concentrations in Banks Peninsula warm spring waters. The Banks Peninsula warm springs are predominantly undersaturated in calcite, exhibiting higher  $\text{Ca}^{2+}$  and  $\text{HCO}_3^{2-}$  concentrations than majority of the Southern Alps hosted tectonic-hydrothermal systems. However, the warm springs do show similar molar values to some Alpine Fault system springs. No correlation is present with Taieri well, the only other known volcanically hosted thermal water outside of Banks Peninsula or the Canterbury aquifer system. (Supplementary data from: Aitchison-Earl et al., 2003; Barnes et al., 1978; Cox et al., 2015; Environment Canterbury, 2014; Hayward, 2002; Reyes et al., 2010).

### 3.2. Water stable isotope chemistry

The Banks Peninsula warm springs plot on the global meteoric water line. The  $\delta^{18}\text{O}$  and  $\delta\text{D}$  signature ranges from  $-8.3$  to  $-9.26$  and  $-60.15$  to  $-64.19$  (‰ V-SMOW), respectively (Fig. 6). The samples indicate the warm spring waters to be of a meteoric origin that exhibit little evidence of evaporation. The warm springs  $\delta^{18}\text{O}$  and  $\delta\text{D}$  signatures are distinct from local groundwater as well as from geochemically similar springs within the TVZ. Instead the warm springs reflect a similar signature to the Waimakariri River, CAS, Alpine Fault System, Marlborough Fault System, and Fiordland Alpine Fault System thermal springs, which are all sourced from meteoric water above the South Island's Southern Alps (Forsyth et al., 2008; Menzies et al., 2016).

$\text{CO}_2$   $\delta^{13}\text{C}$  values of the Banks Peninsula warm springs range from  $-12.37$  to  $-15.06$  (‰ V-PDB; Fig. 7). The warm springs plot within the region of metamorphic hydrothermal systems, differing from magmatic values (Donnelly-Nolan et al., 1993; Griffin, 2016). These results show the influence of tectonically derived metamorphic water mixing with the infiltrating meteoric water at depth (Craw et al., 2013; Horton et al., 2001). The trends shown in Fig. 7 show the springs to have some mixing with the CAS, but do not exhibit the biogenic-atmospheric mixing of the Waimakariri River or the CAS itself (Griffin, 2016). This mixing between the warm springs' water source and the CAS reflects the warm springs' geographical location and the permeability of the local geology, this type of mixing trend is also observed within the 'The Geysers' metamorphic hydrothermal geothermal field, California, U.S.A. (Donnelly-Nolan et al., 1993; Thompson et al., 1976).

### 3.3. Rapaki Bay soil gas flux

Carbon dioxide ( $\text{CO}_2$ ) and methane ( $\text{CH}_4$ ) were detected at the Rapaki Bay site. Under half (31%) of the sampled sites exhibited a  $\text{CO}_2$  flux  $> 0.1 \text{ gm}^{-2} \text{ day}^{-1}$ , which were deemed have a 'positive flux.' Of these positive flux sites 70% produced a flux  $< 5 \text{ gm}^{-2} \text{ day}^{-1}$  (Fig. 8) revealing a strong correlation between areas of higher flux and the position of the warm springs.

The  $\text{CO}_2$  flux averaged at  $6.93 \pm 10 \text{ gm}^{-2} \text{ day}^{-1}$ ,  $\delta^{13}\text{C} -19.81 \pm 5\%$  V-PDB with the highest flux measured at  $39.69 \pm 6 \text{ gm}^{-2} \text{ day}^{-1}$ . Isotopically, the measured  $\text{CO}_2$  fluxes are not distinguished by any biogenic, atmospheric, or magmatic signature. These values plot towards the lower end of a magmatic hydrothermal source; consistent with data from the Wanganui warm spring (Alpine Fault System; Griffin, 2016; Matt Hanson *pers. comm.*) and with a high flux than was measured by Hoke et al. (2000).

$\text{CH}_4$  was also observed during the survey, averaging  $5.58 \pm 12 \text{ gm}^{-2} \text{ day}^{-1}$  with a  $\delta^{13}\text{C}$  signature of  $-59.52 \pm 1$ . The distribution of  $\text{CH}_4$  was highly localised, with positive flux values measured at or close to the surficial expressions of the springs. This is reflective of  $\text{CH}_4$  being a less diffuse gas than  $\text{CO}_2$  (Bloomberg et al., 2014; Giggerbach et al., 1993; Hanson et al., 2014).

### 3.4. Pre-existing faults and seismic effects on the Banks Peninsula warm springs

The CES induced notable effects to groundwater and its behaviour within the Canterbury region affecting areas as far inland as

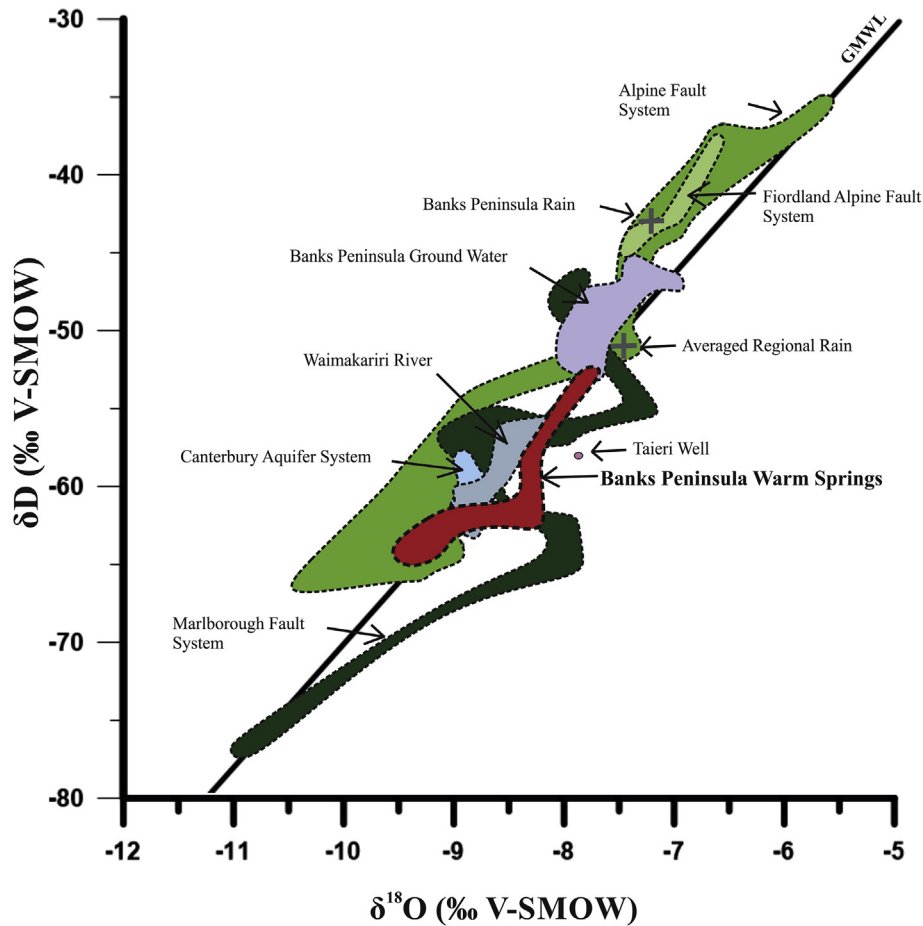


**Fig. 6.** Origin of Banks Peninsula warm spring waters. Banks Peninsula (BP) warm springs (red) plot on the global mean water line (GMWL) indicating a high altitude meteoric source of the warm spring's water similar to the regional ground water (Canterbury Aquifer System) and its main recharge source (Waimakariri River). Other indicated regions are as follows: local groundwater (B.P. gw; purple), averaged local and regional rain (grey cross; *n.b.* sea spray influence in B.P. rain), Alpine Fault System thermal springs (green), Marlborough Fault System thermal springs (dark green), Fiordland Alpine Fault System thermal springs (light green), Canterbury Aquifer System (CAS; blue), Waimakariri River (blue-grey), and the Taieri well (pink). (Supplementary data from: Barnes et al., 1978; Cox et al., 2015; Donnelly-Nolan et al., 1993; Menzies et al., 2014; Reyes et al., 2010; Scott, 2014; Stewart, 2012). (For interpretation of the references to colour in this figure legend, the reader is referred to the web version of this article.)

the Southern Alps (Cox et al., 2015). Around Banks Peninsula, reports surfaced of the warm springs' increased activity and temperature, alongside the notable expansion of the established warm springs' surface features (Griffin, 2016; van Ballegooy et al., 2013). Additionally, new springs within the Hillsborough Valley region appeared (Fig. 1B).

These newly formed north-western Hillsborough Valley springs were coincident with the initial February 22, 2011, Mw 6.2 earthquake event. The springs appeared throughout the valley along fissure tracks generated from the resultant ground movement of the nearby buried fault (Fig. 1B; Green, 2015; Griffin, 2016). The generation of these springs exposed the fault induced fissures as permeable conduits for the hydrothermal systems' fluid flow. The use of faults within Banks Peninsula as a structural control is not new. Hampton (2010) recognised the volcanic growth of the Banks Peninsula volcanics; especially the Lyttelton Volcanics (i.e., where the Banks Peninsula warm springs are located) was controlled by pre-existing faulting within the basement terrane. This structural control relationship between faulting and fluid flow observed at Hillsborough Valley can be applied to the near linear expansion of warm springs observed at both the Motukarara and Rapaki Bay sites (Fig. 8). As a result of the CES, these sites have expanded from a single well-documented spring to a series of quasi-linear related springs (Griffin, 2016), implying an underlying structural control on

the system's fluid transportation.

Pre-existing faults within the host rock are well known to act as conduits for hydrothermal fluid flow (Craw et al., 2013; Horton et al., 2001; Koons et al., 1998; Menzies, 2014). Changes in the stress and strain present within faults/fault systems have been shown to affect the permeability of the system (Anderson, 2005; Tenthorey and Fitz Gerald, 2006). Increased gaseous activity, flow, and temperature, albeit temporarily, can reflect changes to the permeability of a hydrothermal system (Werner and Cardellini, 2006). The appearance of the Hillsborough Valley springs and the reported expansion and increased gaseous activity of the warm springs post CES by locals; provided evidence of permeability change and structural constraint within the Banks Peninsula hydrothermal system. This change in permeability is furthered by the difference in recorded temperatures for both the Motukarara and Rapaki Bay sites and the increased CO<sub>2</sub> gas flux at Rapaki Bay between this study and studies completed prior to the CES (Brown and Weeber, 1994; Craw et al., 2013; Hoke et al., 2000; Reyes et al., 2010). These observed changes to the Banks Peninsula system were also observed in Alpine Fault System springs as a result of the same CES event. Taking into account the evidence provided by the CES; credence can be given to the Sewell et al. (1992) interpretation for fault driven constraint on the Banks Peninsula hydrothermal system. However, the exact relationship between pre-



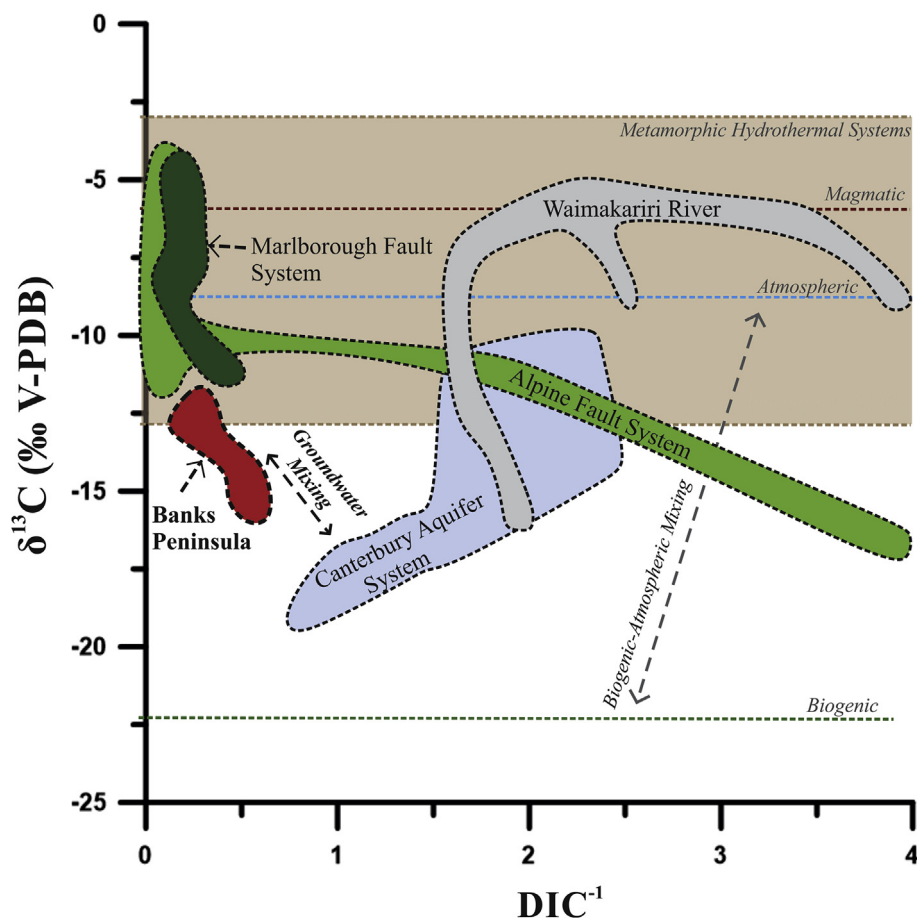


**Fig. 7.** Heat signature of South Island hydrothermal systems. The reciprocal of dissolved inorganic carbon (DIC) when plotted against the waters' measured  $\delta^{13}\text{C}$  indicates the different regions of heat source for the hydrothermal waters. The Banks Peninsula warm springs (B.P., red; this study) plots within Metamorphic Hydrothermal System (MHS) region, just below the Alpine, Marlborough, and Fiordland Alpine Fault Systems (green, dark green, light green; Barnes et al., 1978; Menzies et al., 2016). Some groundwater mixing is evident with Canterbury Aquifer System (CAS; i.e. regional groundwater; blue; Stewart, 2012). This is especially apparent within the newly formed B.P. Hillsborough Valley samples as indicated by the groundwater mixing line. The B.P. samples do not exhibit biogenic-atmospheric mixing nor plot near the Taieri well (pink), a remnant mantle He heat sourced well (Hoke et al., 2000; Reyes et al., 2010). The heat source of the Banks Peninsula warm springs is distinct from the Waimakariri River (the regions dominate groundwater recharge source; blue-grey; Stewart, 2012) and the CAS despite both systems plotting within a similar  $\delta^{18}\text{O}$  and  $\delta\text{D}$  range (Fig. 7). (For interpretation of the references to colour in this figure legend, the reader is referred to the web version of this article.)

existing faults and fractures present in the Rakaia terrane and Banks Peninsula Volcanic Complex with respect to permeability and fluid transportation is an area that requires further investigation.

### 3.5. Tectonic-hydrothermal drivers of Banks Peninsula warm springs

The Southern Alps hosts both irregular fracture-controlled (Alpine Fault and Fiordland Alpine Fault) and strike-slip fault-controlled (Marlborough Fault System) tectonic-hydrothermal systems. All of these hydrothermal systems are fed from meteoric water that has interacted with the metamorphic dehydration fluids associated with the Australian-Pacific boundary collisional zone. This mixed meteoric-metamorphic fluid exploits the local fractures and faults present within the basement terrane as a permeable pathway for fluid flow (Campbell et al., 2004; Cox et al., 2015, 1997; Menzies et al., 2016, 2014; Toy et al., 2015; Wannamaker, 2002).

The main difference between the tectonic-hydrothermal systems located elsewhere on the South Island and the warm springs at Banks Peninsula is the latter's distance from the Australian-Pacific plate-boundary (~150 km). This horizontal distance is significant when compared to the ~5–10 km vertical source to surface

distance reported for the Southern Alps hosted hydrothermal systems (Campbell et al., 2004; Koons and Craw, 1991; Menzies et al., 2014). However, the anomalously low  $\delta^{18}\text{O}$  and  $\delta\text{D}$  values measured at the Banks Peninsula warm springs demonstrate that the emitted fluids cannot be sourced from local meteoric recharge. To the contrary, the only plausible source for the Banks Peninsula spring water is the Southern Alps, the same recharge source that is known to drive the plate-boundary spring systems through topographically driven upper-crustal fluid flow. The stable hydrogen and oxygen isotope data, in conjunction with the springs'  $\delta^{13}\text{C}$  values, suggest that the Banks Peninsula hydrothermal springs are derived from a similar, if not the same, source (Koons et al., 1998; Upton et al., 1995).

The waters from Banks Peninsula occur within an elevated He region (Hoke et al., 2000). These high He levels in conjunction with the springs physical location within the Banks Peninsula volcanics has led to the assumption that the warm springs were heated from either a local remnant shallow mantle melt source similar to what is proposed for Taieri well, Dunedin (Fig. 1A; Hoke et al., 2000) or through complex circulation of old local meteoric waters interacting with the Banks Peninsula volcanics and the upper-mantle (Brown and Weeber, 1994; Reyes et al., 2010). However, despite Banks Peninsula's He concentration being elevated above

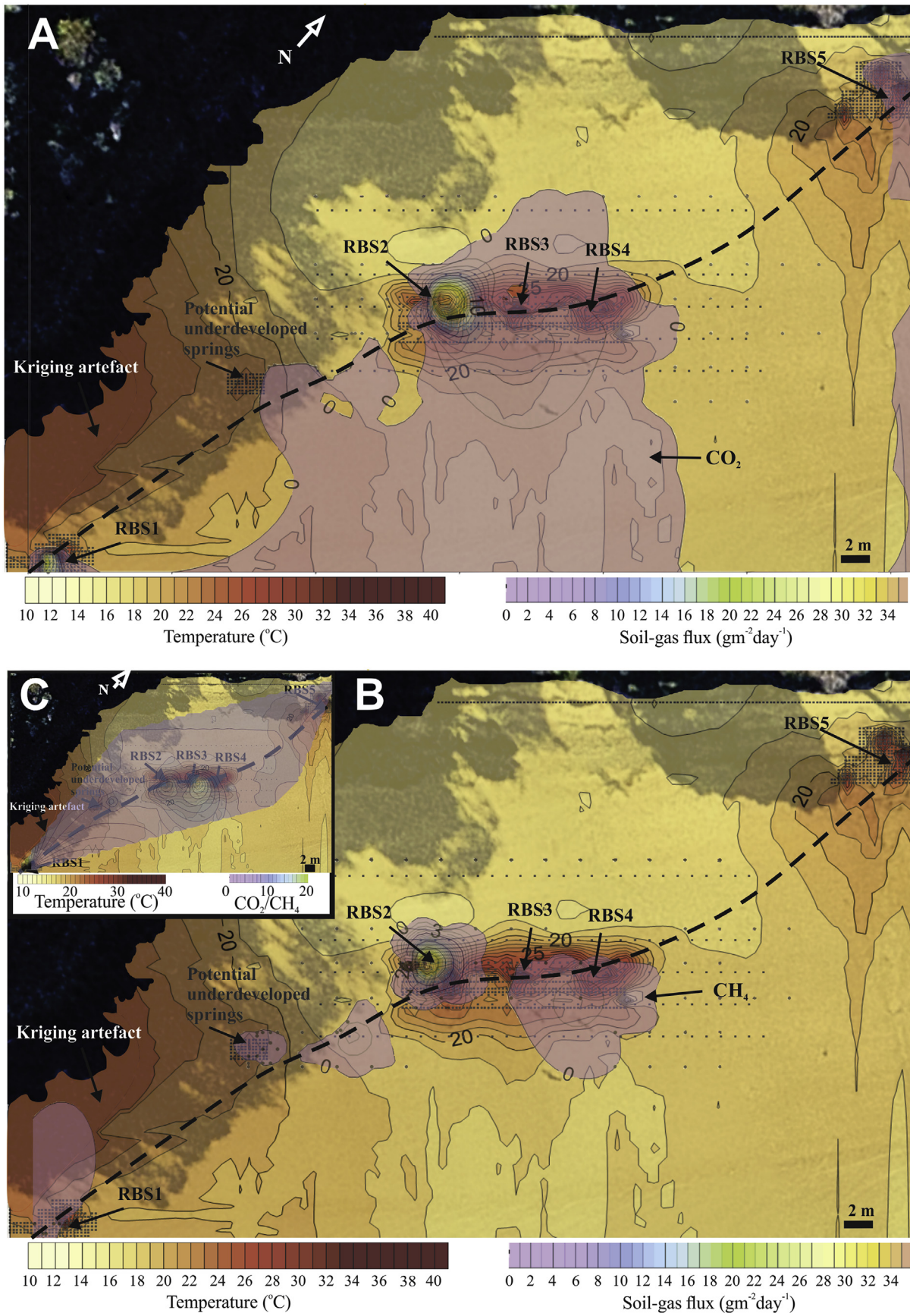


**Fig. 8.** Results of the combined Rapaki Bay soil gas flux and temperature survey. Grey dots indicate soil gas flux sample locations. High soil gas and temperature is closely associated to the labelled warm springs' location (RBS1-RBS5). A) CO<sub>2</sub> soil gas flux data survey. The CO<sub>2(g)</sub> data showcases the connectivity between the different Rapaki Bay springs providing evidence towards a fault driven mechanism. High soil gas flux is measured in close proximity to and between the warm springs, with higher levels also present in areas covered by the SE spring runoff. The inferred sub-surface fault trace (dashed) depicts a quasi-linear relationship between the springs based on the soil gas survey data. B) CH<sub>4</sub> soil gas flux data survey. A less diffuse gas than CO<sub>2</sub>, CH<sub>4</sub> is restricted to the surficial expressions of the Rapaki Bay springs. Where CH<sub>4</sub> is present, a high ratio is present (insert). This high ratio level is unique for the Banks Peninsula springs, with majority of studied South Island thermal springs exhibiting low to undetected CH<sub>4(g)</sub>.



that of other South Island thermal springs, the percentage of mantle He is far lower than what is observed at Dunedin's Taieri well (Hoke et al., 2000). In fact, the Banks Peninsula warm springs mantle He values are within the ranges observed at other Southern Alps-driven springs. This reported percentage mantle He within the Banks Peninsula warm springs, in addition to the springs' geochemical dissimilarity to the Taieri well (Figs. 3–6), makes the original hypotheses of a remnant mantle melt heat source influencing the warm springs or a localised complex deep circulation system less plausible than our hypothesis of the collisional tectonic boundary derived hydrothermal fluid travelling eastward.

Another factor to consider when addressing the Banks Peninsula warm springs as part of the collisional zone sourced hydrothermal systems of the South Island is the presence of the CAS. The CAS is an extensive aquifer system, predominantly hosted within the overlying Pleistocene sediment, between Banks Peninsula and the Southern Alps. Evidence of some mixing between the CAS and the Banks Peninsula warm springs is observable within the  $\delta^{13}\text{C}$  values of the northwestern (Hillsborough Valley) warm spring samples (HVS1-2 Table 1; Fig. 7). This reflects the northwestern springs' geographical position on the outerflanks of the volcanic edifice and their subsequent susceptibility to groundwater influence from the overlapping CAS, resulting from the thick overburden of loess (Green, 2015; Griffin, 2016). However, the lack of CAS influence present within the Rapaki Bay samples suggests these thermal waters follow an isolated path that does not intersect the CAS. This hypothesis is further validated by the presence of thermal wells encountered at depth within the Canterbury region (Brown and Weeber, 1994). The exact mechanism for the transport of this hydrothermal fluid and its relationship to pre-existing faults within the Rakaia terrane is an area that is not addressed in this paper, but is an area that requires further investigation.

A similarity between the tectonic-hydrothermal systems of the Southern Alps and the warm springs of Banks Peninsula is evident. Both systems are connected by the basement Rakaia terrane and plot isotopically and geochemically within the same regions. The Banks Peninsula warm springs exhibit very little correlation to geochemically similar springs within the North Island's TVZ hydrothermal system or the mantle heated Taieri well in Dunedin (Hanson et al., 2014; Reyes et al., 2010; Rissmann et al., 2012; Werner and Cardellini, 2006). From this study, the Banks Peninsula warm springs are shown to exhibit geochemical patterns that are indicative of a tectonically driven metamorphic heated hydrothermal system, reflecting geochemical trends that are also observed within the other South Island thermal springs associated with the Australian-Pacific plate boundary collisional zone (Barnes et al., 1978; Cox et al., 2015; Menzies et al., 2016; Reyes et al., 2010).

#### 4. Conclusions

Aqueous and gaseous geochemical data is consistent with the hypothesis that the Banks Peninsula warm springs, South Island, New Zealand, are sourced from a tectonic-hydrothermal system composed of mixed high-altitude meteoric-derived water and metamorphic fluids. Such hydrothermal systems dominate upper-crustal fluid flow across the South Island due to the presence of the convergent Australian-Pacific plate boundary system. Based on the geochemical data presented, we suggest that the warm spring systems on Banks Peninsula represent an outboard extension of the Southern Alps hydrothermal systems, rather than its own independent low-enthalpy hydrothermal system. Canterbury Earthquake Sequence induced perturbations to the pre-existing Banks Peninsula warm springs at Rapaki Bay and elsewhere, in conjunction with the formation of the Hillsborough Valley warm springs, demonstrate an intimate structural control along the flow path of

these anomalous springs from their montane recharge zone to their coastal discharge sites.

#### Acknowledgements

We are thankful to the property owners who allowed us access to the springs. Matt Hanson for his sharing his knowledge and data. Matt, Melanie, and Nicky for their assistance in the field. The University of Canterbury Chemistry Department for access and assistance with analytical equipment, and The University of Canterbury's Mason Trust for supporting this research. The authors would also like to thank Dave Craw and another anonymous reviewer for their comments which significantly enhanced this manuscript.

#### References

- Aitchison-Earl, P., Ettema, M., Hanson, C., Hayward, S., Larking, R., Sanders, R., Scott, D., Veltman, A., 2003. Report No. R04/18: Coastal Aquifer Saltwater Intrusion Assessment Guidelines (Christchurch).
- Anderson, M.P., 2005. Heat as a ground water tracer. *Ground Water* 43, 951–968. <https://doi.org/10.1111/j.1745-6584.2005.00052.x>.
- Barnes, I., Downes, C.J., Hulston, J.R., 1978. Warm springs, South Island, New Zealand, and their potentials to yield laumontite. *Am. J. Sci.* 278, 1412–1427. <https://doi.org/10.2475/ajs.278.10.1412>.
- Beavan, J., Fielding, E., Motagh, M., Samsonov, S., Donnelly, N., 2011. Fault location and slip distribution of the 22 February 2011 Mw 6.2 Christchurch, New Zealand, earthquake from geodetic data. *Seismol. Res. Lett.* 82, 789–799. <https://doi.org/10.1785/gssrl.82.6.789>.
- Beysac, O., Cox, S.C., Vry, J., Herman, F., 2016. Peak metamorphic temperature and thermal history of the Southern Alps (New Zealand). *Tectonophysics* 676, 229–249. <https://doi.org/10.1016/j.tecto.2015.12.024>.
- Bloomberg, S., Werner, C., Rissmann, C., Mazot, A., Horton, T., Graveley, D., Kennedy, B., Oze, C., 2014. Soil CO<sub>2</sub> emissions as a proxy for heat and mass flow assessment, Taupo Volcanic Zone, New Zealand. *Geochemistry, Geophys. Systems* G3 15, 4885–4904. <https://doi.org/10.1002/2014GC005327>. Received.
- Brown, L.J., Beetham, R.D., Paterson, B.R., Weeber, J.H., 1995. *Geology of Christchurch, New Zealand*. *Environ. Eng. Geosci.* 1, 427–488.
- Brown, L.J., Weeber, J.H., 1994. Hydrogeological implications of geology at the boundary of Banks Peninsula volcanic rock aquifers and Canterbury Plains fluvial gravel aquifers. *New zeal. J. Geol. geophys.* 37, 181–193. <https://doi.org/10.1080/00288306.1994.9514613>.
- Campbell, J.R., Craw, D., Frew, R., Horton, T., Chamberlain, C.P., 2004. Geochemical signature of orogenic hydrothermal activity in an active tectonic intersection zone, Alpine Fault, New Zealand. *Min. Depos.* 39, 437–451. <https://doi.org/10.1007/s00126-004-0421-4>.
- Chiodini, G., Cioni, R., Guidi, M., Raco, B., Marini, L., 1998. Soil CO<sub>2</sub> flux measurements in volcanic and geothermal areas. *Appl. Geochem.* 13, 543–552. [https://doi.org/10.1016/S0883-2927\(97\)00076-0](https://doi.org/10.1016/S0883-2927(97)00076-0).
- Cox, S.C., Craw, D., Chamberlain, C.P., 1997. Structure and fluid migration in a late Cenozoic duplex system forming the Main Divide in the central Southern Alps, New Zealand. *New zeal. J. Geol. geophys.* 40, 359–373. <https://doi.org/10.1080/00288306.1997.9514767>.
- Cox, S.C., Menzies, C.D., Sutherland, R., Denys, P.H., Chamberlain, C., Teagle, D. A. H., 2015. Changes in hot spring temperature and hydrogeology of the Alpine Fault hanging wall, New Zealand, induced by distal South Island earthquakes. *Geofluids* 15, 216–239. <https://doi.org/10.1111/gfl.12093>.
- Craw, D., Upton, P., Horton, T., Williams, J., 2013. Migration of hydrothermal systems in an evolving collisional orogen, New Zealand. *Min. Depos.* 48, 233–248. <https://doi.org/10.1007/s00126-012-0421-8>.
- Donnelly-Nolan, J.M., Burns, M.G., Goff, F.E., Peters, E.K., Thompson, J.M., 1993. The Geysers-Clear Lake area, California: thermal waters, mineralization, volcanism, and geothermal potential. *Econ. Geol.* 88, 301–316. <https://doi.org/10.2113/gsecongeo.88.2.301>.
- Environment Canterbury, G.Q.T., 2014. Report No. R14/68: Christchurch Groundwater Quality Monitoring 2013. Christchurch.
- Forsyth, P.J., Barrell, D.J.A., Jongens, R., 2008. In: *Geology of the Christchurch Area*, 1: 250 000. Institute of Geological & Nuclear Sciences Ltd., Lower Hutt, New Zealand.
- Giggenbach, W., Sano, Y., Wakita, H., 1993. Isotopic composition of helium, and CO<sub>2</sub> and CH<sub>4</sub> contents in gases produced along the New Zealand part of a convergent plate boundary. *Geochim. Cosmochim. Acta* 57, 3427–3455. [https://doi.org/10.1016/0016-7037\(93\)90549-C](https://doi.org/10.1016/0016-7037(93)90549-C).
- Green, M., 2015. *Hydrogeological Investigation of Earthquake Related Springs in the Hillsborough Valley*. University of Canterbury, Christchurch, New Zealand.
- Griffin, S.N., 2016. *Geochemical Tracing of the Source of Water Dissolved Inorganic Carbon and Chloride in Banks Peninsula Warm Springs*. University of Canterbury, New Zealand.
- Griffiths, E., 1973. Loess of Banks peninsula. *New zeal. J. Geol. geophys.* 16, 657–675. <https://doi.org/10.1080/00288306.1973.10431388>.

- Guglielmetti, L., Comina, C., Abdelfettah, Y., Schill, E., Mandrone, G., 2013. Integration of 3D geological modeling and gravity surveys for geothermal prospection in an Alpine region. *Tectonophysics* 608, 1025–1036.
- Hampton, S., Cole, J., Bell, D., 2012. Syn-eruptive alluvial and fluvial volcanogenic systems within an eroding Miocene volcanic complex, Lyttelton Volcano, Banks Peninsula, New Zealand. *New Zeal. J. Geol. geophys.* 55, 53–66. <https://doi.org/10.1080/00288306.2011.632424>.
- Hampton, S.J., 2010. Growth, Structure and Evolution of the Lyttelton Volcanic Complex, Banks Peninsula. University of Canterbury, New Zealand.
- Hanson, M., Oze, C., Horton, T.W., 2014. Identifying blind geothermal systems with CO<sub>2</sub> surveys. *Appl. Geochem.* 50, 106–114. <https://doi.org/10.1016/j.apgeochem.2014.08.009>.
- Hayward, S. a., 2002. Report No. U02/47 Part II: Christchurch-west Melton Groundwater Quality: a Review of Groundwater Quality Monitoring Data from January 1986 to March 2002. Christchurch.
- Hoke, L., Poreda, R., Reay, a., Weaver, S.D., 2000. The subcontinental mantle beneath southern New Zealand, characterised by helium isotopes in intraplate basalts and gas-rich springs. *Geochim. Cosmochim. Acta* 64, 2489–2507. [https://doi.org/10.1016/S0016-7037\(00\)00346-X](https://doi.org/10.1016/S0016-7037(00)00346-X).
- Horton, T.W., Becker, J. a., Craw, D., Koons, P.O., Chamberlain, C.P., 2001. Hydrothermal arsenic enrichment in an active mountain belt: southern Alps. *New Zeal. Chem. Geol.* 177, 323–339. [https://doi.org/10.1016/S0009-2541\(00\)00416-2](https://doi.org/10.1016/S0009-2541(00)00416-2).
- Kaiser, A., Holden, C., Beavan, J., Beetham, D., Benites, R., Celentano, A., Collett, D., Cousins, J., Cubrinovski, M., Dellow, G., Denys, P., Fielding, E., Fry, B., Gerstenberger, M., Langridge, R., Massey, C., Motagh, M., Pondard, N., McVerry, G., Ristau, J., Stirling, M., Thomas, J., Uma, S., Zhao, J., 2012. 6.2 Christchurch earthquake of February 2011: preliminary report. *New Zeal. J. Geol. geophys.* 55, 67–90. <https://doi.org/10.1080/00288306.2011.641182>.
- Koons, P.O., Craw, D., 1991. Evolution of fluid driving forces and composition within collisional orogens. *Geophys. Res. Lett.* 18, 935–938.
- Koons, P.O., Craw, D., Cox, S.C., Upton, P., Templeton, A.S., Chamberlain, C.P., 1998. Fluid flow during active oblique convergence: a Southern Alps model from mechanical and geochemical observations. *Geology* 26, 159–162. [https://doi.org/10.1130/0091-7613\(1998\)026<0159:FFDAOC>2.3.CO;2](https://doi.org/10.1130/0091-7613(1998)026<0159:FFDAOC>2.3.CO;2).
- Menzies, C.D., 2014. Incursion of meteoric waters into the ductile regime in an active orogen - supplementary data. *Earth Planet. Sci. Lett.* 399. Supplementary data.
- Menzies, C.D., Teagle, D.A.H., Craw, D., Cox, S.C., Boyce, A.J., Barrie, C.D., Roberts, S., 2014. Incursion of meteoric waters into the ductile regime in an active orogen. *Earth Planet. Sci. Lett.* 399, 1–13. <https://doi.org/10.1016/j.epsl.2014.04.046>.
- Menzies, C.D., Teagle, D.A.H., Niedermann, S., Cox, S.C., Craw, D., Zimmer, M., Cooper, M.J., Erzinger, J., 2016. The fluid budget of a continental plate boundary fault: quantification from the Alpine Fault, New Zealand. *Earth Planet. Sci. Lett.* 445, 125–135. <https://doi.org/10.1016/j.epsl.2016.03.046>.
- Mortimer, N., 2004. New Zealand's geological foundations. *Gondwana Res.* 7, 261–272. [https://doi.org/10.1016/S1342-937X\(05\)70324-5](https://doi.org/10.1016/S1342-937X(05)70324-5).
- Quigley, M.C., Hughes, M.W., Bradley, B.A., van Ballegooy, S., Reid, C., Morgenroth, J., Horton, T., Duffy, B., Pettinga, J.R., 2016. The 2010–2011 Canterbury Earthquake Sequence: environmental effects, seismic triggering thresholds and geologic legacy. *Tectonophysics* 672–673, 228–274. <https://doi.org/10.1016/j.tecto.2016.01.044>.
- Reyes, A., Jongens, R., 2005. Tectonic settings of low enthalpy geothermal systems in New Zealand: an overview. In: *Proceedings World Geothermal Congress*, pp. 24–29.
- Reyes, A.G., Britten, K., 2007. Variations in Chemical and Isotopic Compositions of Mineral Spring Systems in South Island, New Zealand, pp. 1–6.
- Reyes, A.G., Christenson, B.W., Faure, K., 2010. Sources of solutes and heat in low-enthalpy mineral waters and their relation to tectonic setting, New Zealand. *J. Volcanol. Geotherm. Res.* 192, 117–141. <https://doi.org/10.1016/j.jvolgeores.2010.02.015>.
- Ring, U., Hampton, S., 2012. Faulting in Banks Peninsula: tectonic setting and structural controls for late Miocene intraplate volcanism, New Zealand. *J. Geol. Soc. Lond.* 169, 773–785. <https://doi.org/10.1144/jgs2011-167>.
- Rissmann, C., Christenson, B., Werner, C., Leybourne, M., Cole, J., Gravley, D., 2012. Surface heat flow and CO<sub>2</sub> emissions within the Ohaaki hydrothermal field, Taupo Volcanic Zone, New Zeal. *Appl. Geochem.* 27, 223–239. <https://doi.org/10.1016/j.apgeochem.2011.10.006>.
- Scott, L., 2014. Report No. R14/128: Review of Environment Canterbury's Groundwater Oxygen-18 Data (Christchurch).
- Sewell, R.J., Weaver, S.D., Reay, M.B., 1992. Geology of Banks Peninsula, Scale 1:10. Ed. Institute of Geological & Nuclear Sciences Ltd, Lower Hutt, New Zealand.
- Spötl, C., 2005. A robust and fast method of sampling and analysis of delta<sup>13</sup>C of dissolved inorganic carbon in ground waters. *Isot. Environ. Health Stud.* 41, 217–221. <https://doi.org/10.1080/10256010500230023>.
- Stewart, M.K., 2012. A 40-year record of carbon-14 and tritium in the Christchurch groundwater system, New Zealand: dating of young samples with carbon-14. *J. Hydrol.* 430–431, 50–68. <https://doi.org/10.1016/j.jhydrol.2012.01.046>.
- Sutherland, R., Townend, J., Toy, V., Upton, P., Coussens, J., Allen, M., Baratin, L.-M., Barth, N., Becroft, L., Boese, C., Boles, A., Boulton, C., Broderick, N.G.R., Janku-Capova, L., Carpenter, B.M., Célérier, B., Chamberlain, C., Cooper, A., Coutts, A., Cox, S., Craw, L., Doan, M.-L., Eccles, J., Faulkner, D., Grieve, J., Grochowski, J., Gulley, A., Hartog, A., Howarth, J., Jacobs, K., Jeppson, T., Kato, N., Keys, S., Kirilova, M., Kometani, Y., Langridge, R., Lin, W., Little, T., Lukacs, A., Mallyon, D., Mariani, E., Massiot, C., Mathewson, L., Melosh, B., Menzies, C., Moore, J., Morales, L., Morgan, C., Mori, H., Niemeijer, A., Nishikawa, O., Prior, D., Sauer, K., Savage, M., Schleicher, A., Schmitt, D.R., Shigematsu, N., Taylor-Offord, S., Teagle, D., Tobin, H., Valdez, R., Weaver, K., Wiersberg, T., Williams, J., Woodman, N., Zimmer, M., 2017. Extreme hydrothermal conditions at an active plate-bounding fault. *Nature* 546, 137–140. <https://doi.org/10.1038/nature22355>.
- Tenthorey, E., Fitz Gerald, J.D., 2006. Feedbacks between deformation, hydrothermal reaction and permeability evolution in the crust: experimental insights. *Earth Planet. Sci. Lett.* 247, 117–129. <https://doi.org/10.1016/j.epsl.2006.05.005>.
- Thain, I., Reyes, A.G., Hunt, T., 2006. A Practical Guide to Exploiting Low Temperature Geothermal Resources.
- Thompson, J.M., Goff, F.E., Donnelly, J.M., 1976. Report 78–425: Chemical Analyses of Waters from Springs and Wells from the Clear Lake Volcanic Area. California, Northern California. Menlo Park. <https://doi.org/10.1007/s13398-014-0173-7.2>.
- Toy, V.G., Boulton, C.J., Sutherland, R., Townend, J., Norris, R.J., Little, T.A., Prior, D.J., Mariani, E., Faulkner, D., Menzies, C.D., Scott, H., Carpenter, B.M., 2015. Fault rock lithologies and architecture of the central Alpine fault, New Zealand, revealed by DFDP-1 drilling. *Lithosphere* 7, 155–173. <https://doi.org/10.1130/L395.1>.
- Upton, P., Koons, P.O., Chamberlain, C.P., 1995. Penetration of deformation-driven meteoric water into ductile rocks: isotopic and model observations from the Southern Alps, New Zealand. *New Zeal. J. Geol. geophys.* 38, 535–543. <https://doi.org/10.1080/00288306.1995.9514680>.
- USGS, 2012. Alkalinity calculator. <https://or.water.usgs.gov/alk/> accessed 24 June 2015.
- USGS, 2013. Methods for alkalinity calculations. <https://or.water.usgs.gov/alk/methods.html> accessed 24 June 2015.
- van Ballegooy, S., Cox, S.C., Agnihotri, R., Reynolds, T., Thurlow, C., Rutter, H.K., Scott, D.M., Begg, J.G., McCahon, I., 2013. Median Water Table Elevation in Christchurch and Surrounding Area after the 4 September 2010. *Darfield Earthquake, Christchurch*.
- Wannamaker, P.E., 2002. Fluid generation and pathways beneath an active compressional orogen, the New Zealand Southern Alps, inferred from magnetotelluric data. *J. Geophys. Res.* 107, 1–21. <https://doi.org/10.1029/2001JB000186>.
- Werner, C., Cardellini, C., 2006. Comparison of carbon dioxide emissions with fluid upflow, chemistry, and geologic structures at the Rotorua geothermal system, New Zealand. *Geothermics* 35, 221–238. <https://doi.org/10.1016/j.geothermics.2006.02.006>.